Nonlinear Optical Properties of Flavylium Salts: A Quantum Chemical Study

ARTICLE *in* THE JOURNAL OF PHYSICAL CHEMISTRY A · AUGUST 2010

Impact Factor: 2.69 · DOI: 10.1021/jp1056804 · Source: PubMed

5 AUTHORS, INCLUDING:

Elena Bogdan
Université de Nantes, Nantes, France
10 PUBLICATIONS **142** CITATIONS
SEE PROFILE

Laurent Ducasse
Université Bordeaux 1
157 PUBLICATIONS **2,607** CITATIONS
SEE PROFILE

Benoît Champagne
University of Namur
401 PUBLICATIONS **8,753** CITATIONS
SEE PROFILE

Frédéric Castet
Université of Bordeaux
90 PUBLICATIONS **1,694** CITATIONS
SEE PROFILE

Nonlinear Optical Properties of Flavylium Salts: A Quantum Chemical Study

Elena Bogdan,[†] Léa Rougier,[†] Laurent Ducasse,[†] Benoît Champagne,[‡] and Frédéric Castet*[,†]

Institut des Sciences Moléculaires, Université de Bordeaux, 351 Cours de la Libération, F-33405 Talence, France and Laboratoire de Chimie Théorique, Facultés Universitaires Notre-Dame de la Paix (FUNDP), 61 Rue de Bruxelles, B-5000 Namur, Belgium

Received: June 20, 2010; Revised Manuscript Received: July 9, 2010

Ab initio calculations have been carried out to unravel the relationships between the structure and the first hyperpolarizability in flavylium derivatives, with the aim to design efficient second-order nonlinear optical (NLO) switching compounds. Large contrasts of the first hyperpolarizability have been obtained along the pH-controlled and photoinduced transformations for specific combinations of chemical substituents in the 4′- and 7-positions, which demonstrates that these multistate systems should behave as highly efficient molecular NLO switches.

1. Introduction

In the recent years, the rapid development of optical telecommunications has greatly increased the demand for high-added value materials for information transport and storage, including systems with commutable nonlinear optical (NLO) responses. Due to their flexibility, as well as their numerous other advantages such as tailored synthesis, low cost, and easy and environment friendly processing, organic materials are highly attractive for optoelectronic applications such as molecular-level memory devices. In this context, the design of organic molecular switches with high NLO contrasts has motivated a lot of experimental and theoretical works.[1]

The potential interest for such NLO switches in view of technological applications results, however, from necessary compromises that overpass the molecular level. Indeed, a large β contrast between the NLO active and inactive form is often accompanied by a significant structural distortion along the transformation, which reduces the commutation efficiency after integration within a rigid matrix. On the contrary, limited structural changes, encountered for instance in the tautomeric equilibrium of Schiff base derivatives, ensure the possibility of switching in the solid state with short commutation times, but concomitantly lower the NLO contrast along the commutation.[2] Note however that a large difference in hyperpolarizability was detected along the light-induced solid-state proton transfer of dinitrobenzyl pyridine derivatives, due to the quasi-total extinction of the NLO response in one of the two stable tautomeric forms.[3]

The improvement of the storage capacity of optical memories as well as the diversification of the addressability of the devices are also challenging tasks, which encompass the design of multistate and multifunctional systems. In that respect, benzazolo-oxazolidine derivatives have been recently shown to be highly promising owing to their ability to commute indifferently by light irradiation or pH variations between two forms displaying very large differences in their second harmonic generation (SHG) responses.[4] As both multistate and multiaddressable systems, flavylium salts also appear as highly attractive for potential uses in NLO applications, although they have never been studied in this context.

SCHEME 1: Structural Transformations of the Flavylium-Type Compounds

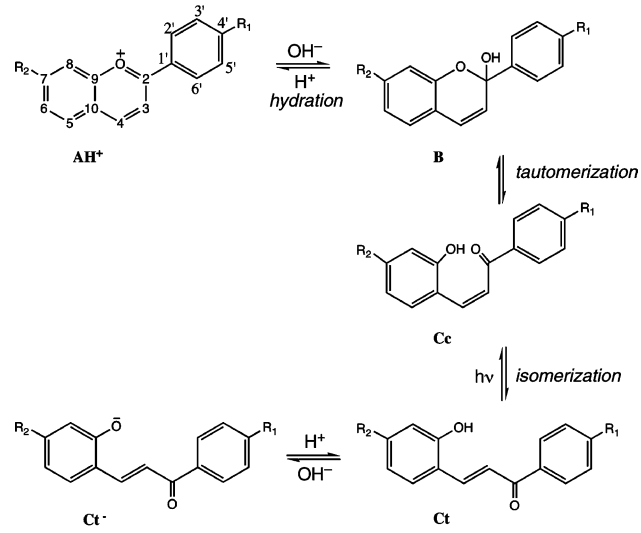

Synthetic flavylium salts possess the basic structure of natural anthocyanins, one of the most important families of natural chromophores responsible for colors in flowers and fruits. In the recent years, the pH-controlled and/or photoinduced transformations of these compounds in aqueous solutions or ionic liquids have stimulated a lot of studies.[5] As shown in Scheme 1, the flavylium cation $\mathbf{AH}^+$ is thermodynamically stable in water in very acidic conditions. Increasing the pH, the hydration of $\mathbf{AH}^+$ leads to the hemiketal species **B** and to its *cis*-chalcone tautomer **Cc** via the hemiketal ring-opening. The **B** and **Cc** forms are short-lived transient species, and convert into the *trans*-chalcone form, **Ct**, owing to the isomerization of **Cc**. Further pH increase leads to the anionic form $\mathbf{Ct}^-$, while the thermally stable *trans*-chalcone **Ct** can be converted reversibly into the **Cc** form upon light irradiation.

Beyond a potential use as light-switchable pH sensors, Pina and co-workers have demonstrated that this complex network of chemical reactions can be taken as a basis in view of applications for data processing and storage, as these multistate/

* To whom correspondence should be addressed. E-mail: f.castet@ism.u-bordeaux1.fr.
[†] Université de Bordeaux.
[‡] Facultés Universitaires Notre-Dame de la Paix.

10.1021/jp1056804
Published on Web 07/22/2010

multifunctional systems can behave as logic devices. In particular, the pH and phototriggered transformations of the 4′-hydroxy- or 4′-methoxyflavylium ions (R_1 = OH or OMe) can be exploited for optical memory systems with multiple storage and nondestructive capacity through *write-lock-read-unlock-erase* cycles.[6] The multistate networks based on the 4′-acetamido- and 4′-aminoflavylium have also been proposed for optical memories operating by different algorithms.[7] In a general way, all these studies have demonstrated that substituents in the 4′- and 7-positions have a strong influence on the thermal and photochemical reactivity of the different forms,[8] as well as solvent effects.[8e,9,10] It has also been demonstrated that flavylium-based systems display photochromism after incorporation in soft materials such as polymer hydrogels,[11] micelles solutions,[12] pluronic gels,[13] and biphasic water/ionic liquid systems.[14]

In this study, we investigate the potential of flavylium salts to display efficient NLO switching properties. Quantum chemical calculations are performed in order to characterize the electronic and second-order NLO properties of the main stable forms $\mathbf{AH}^+$, **Ct** and $\mathbf{Ct}^-$, as a function of the R_1 and R_2 substituents grafted at the 4′- and 7-positions.

2. Computational Aspects

The molecular structures have been optimized in vacuo at the B3LYP/6-311G(d) level and were found to be true minima on the basis of their harmonic vibrational frequencies. Time-dependent DFT (TDDFT) calculations were carried out with the same exchange-correlation functional and basis set to determine the vertical excitation energies and the excited state properties of the compounds. The coupled-perturbed Hartree−Fock (CPHF) and the time-dependent Hartree−Fock (TDHF)[15] schemes were respectively applied for obtaining static and dynamic first hyperpolarizabilities, using an incident wavelength of 1064 nm. Solvent effects were included using the polarizable continuum model within the integral equation formalism (IEF-PCM),[16] by taking $\epsilon_0 = 36.640$ ($\epsilon_\infty = 1.806$) for acetonitrile, which is a typical solvent used in NLO measurements. To account for correlation effects, the second-order Møller−Plesset (MP2) method was employed in combination with the finite field (FF) procedure[17] implying a Romberg scheme to improve the accuracy on the numerical derivatives.[18] FF/MP2 calculations were already shown to provide reliable first hyperpolarizabilities for organic chromophores.[2e,4] Moreover, in many cases, the MP2 method recovers the largest part of the electron correlation effects, as estimated from higher-order methods.[19] Frequency dispersion effects were then estimated by adopting the percentage or multiplicative correction scheme, which has been shown to be suitable for different systems:[2e,4]

$$\beta_{MP2}(-2\omega;\omega,\omega) \approx \beta_{MP2}(0;0,0) \times \frac{\beta_{TDHF}(-2\omega;\omega,\omega)}{\beta_{CPHF}(0;0,0)} \quad (1)$$

The hyper-Rayleigh scattering (HRS) responses were analyzed, since HRS is the technique of choice to probe the first hyperpolarizability of charged molecules.[20] In the case of plane-polarized incident light and observation made perpendicular to the propagation plane without polarization analysis of the scattered beam, the second-order NLO response that can be extracted from HRS data reads:

$$\beta_{HRS}(-2\omega;\omega,\omega) = \sqrt{\{\langle\beta^2_{ZZZ}\rangle + \langle\beta^2_{ZXX}\rangle\}} \quad (2)$$

where $\langle\beta^2_{ZZZ}\rangle$ and $\langle\beta^2_{ZXX}\rangle$ correspond to orientational averages of the molecular β tensor components.[21] The associated depolarization ratio is given by:

$$DR = \frac{\langle\beta^2_{ZZZ}\rangle}{\langle\beta^2_{ZXX}\rangle} \quad (3)$$

The depolarization ratio gives information on the geometry of the part of the molecule responsible for the NLO response (for an ideal donor/acceptor 1D system DR = 5, for an octupolar molecule, DR = 1.5 whereas for a Λ-shape molecule, the amplitude of DR depends on the angle between the chromophore as well as on the D/A groups[22]). All calculations were performed with Gaussian 03.[23]

3. Molecular Structures

The molecular structures have been optimized at the B3LYP/6-311G(d) level in the gas phase. The main geometrical features (distances, angles, and dihedral angles) of the $\mathbf{AH}^+$, **Cc**, **Ct**, and $\mathbf{Ct}^-$ forms are collected in Tables S1a−d (Supporting Information). As indicators for the strength of the electron delocalization along the compounds, Tables S1 also report the bond length alternations (BLA) in the central part of the molecules, defined as:

$$BLA_1 = (d_{10-4} + d_{3-2} - 2d_{4-3})/2$$

$$BLA_2 = (d_{4-3} + d_{2-1'} - 2d_{3-2})/2$$

$$BLA_3 = (d_{3-2} + d_{1'-2'} - 2d_{2-1'})/2$$

It is found that the BLAs strongly differ from one chemical form to the other. As expected from the Lewis structures, the largest degree of conjugation (associated to the smallest BLAs) is obtained for the $\mathbf{AH}^+$ form. The three thermally stable forms ($\mathbf{AH}^+$, **Ct**, and $\mathbf{Ct}^-$) display planar (or nearly planar) geometries, as indicated by the values of the four representative dihedral angles gathered in Tables S1a−d. Note, however, that the 3−2−1′−2′ angles deviate from 180° by 10−15° for the $\mathbf{AH}^+$ and **Ct** forms with $R_1 = NO_2$. Not surprisingly, the **Cc** forms display larger distortions, although these forms are stabilized by an intramolecular hydrogen bond between the carbonyl oxygen and the hydrogen of the hydroxy group in 9-position.

Table 1 reports the Gibbs free energy differences at 298.15 K between the **Cc** and **Ct** forms, $\Delta G = G(\mathbf{Cc}) - G(\mathbf{Ct})$. The relative stability of these two forms—as well as the energy barriers between them—is one of the key aspects for a potential use of these systems as optical memory devices with nondestructive readout capacity, since it dictates the relative rate constants of the *cis* → *trans* isomerization and of the competing reverse reaction leading from **Cc** to $\mathbf{AH}^+$.[5d] For all the compounds, DFT calculations predict that the **Ct** form is more stable than **Cc**. Consistently with previous experimental and theoretical observations,[5c,d,6a,b,8a,f] the energy of the *cis* → *trans* isomerization is significantly impacted by the nature of the R_1 and R_2 substituents, with ΔG values ranging from 0.84 kJ/mol (for R_1 = OH and $R_2 = NMe_2$) to 11.92 kJ/mol (for $R_1 = NO_2$ and R_2 = H). Smaller ΔG values are obtained when the R_1 and/or R_2 substituents are strong donors (NH_2, NMe_2).

TABLE 1: Relative Gibbs Free Energies of the Cc and Ct Forms ($\Delta G = G_{Cc} - G_{Ct}$, kJ/mol) Calculated at the B3LYP/6-311G(d) Level in the Gas Phase

R_1	R_2	ΔG
H	H	7.16
H	OH	5.69
OH	H	7.05
OH	OCH_3	8.38
OH	OH	6.31
OH	NH_2	1.62
OH	NMe_2	0.84
OH	NO_2	8.56
OH	CN	7.12
NMe_2	H	4.82
NMe_2	NO_2	4.88
OCH_3	H	6.08
OCH_3	NO_2	7.84
NO_2	H	11.92
NO_2	NMe_2	4.37
NO_2	OCH_3	10.66

4. Linear Optical Properties

Table S2 gathers the transition energies, ΔE_{ge}, wavelengths, λ_{ge}, and oscillator strengths, f_{ge}, associated to the main low-energy optical transitions calculated in acetonitrile solution for $\mathbf{AH}^+$, **Ct**, and $\mathbf{Ct}^-$ forms with different substituents. The nature of the molecular orbitals (MOs) involved in these transitions is also given. The frontier MOs of the compounds (issued from AM1 calculations) are depicted in Figure S1, while the absorption spectra simulated at the IEFPCM/B3LYP/6-311G(d) level are given in Figure S2.

For the $\mathbf{AH}^+$ forms, the main absorption band is associated to a $\pi \rightarrow \pi^*$ transition between the highest occupied (HOMO, H) and the lowest unoccupied (LUMO, L) molecular orbitals. The excitation wavelengths strongly depend on the R_1 and R_2 substituents, in good agreement with the available experimental data, except when $R_1 = NMe_2$ and $R_2 = H$ (see Table S2). In this case, theoretical simulations underestimate the maximum absorption wavelength of $\mathbf{AH}^+$, and consequently the bathochromic shift accompanying the hydration reaction $\mathbf{AH}^+ \rightarrow \mathbf{Ct}$. Additional calculations performed using the long-range corrected LC-BLYP functional show an improved agreement with the observed bathochromic shift (109 nm). Besides, one should note that only UV/visible measurements performed in acetonitrile are directly comparable to our calculations, since significant solvatochromism is observed.

Regarding the substituent effects in the $\mathbf{AH}^+$ forms, the smaller wavelengths are obtained for the unsubstituted compound (382 nm) and for the 4′-nitro-flavylium (380 nm). In the latter compound, the electron withdrawing effects of the nitro group in 4′-position are annihilated due to competition with the electron-deficient oxygen atom, as evidenced by the shape of the frontier MOs, which does not change upon substitution. On the contrary, the addition of a π-donor group in R_1 increases the electron delocalization, and thus the absorption wavelength to 414 nm for the 4′-hydroxy-flavylium, to 417 nm for the 4′-methoxy-flavylium, and to 467 nm for the 4′-dimethylamino-flavylium. The addition of an acceptor group in R_2 (while keeping a donor group in R_1) further increases the wavelength due to a significant photoinduced charge transfer from the phenyl to the benzopyrylium group, as shown by the HOMO and LUMO densities. For example, the $S_0 \rightarrow S_1$ transition is found at 456 nm with $[R_1, R_2] = [OCH_3, NO_2]$ and at 535 nm with $[R_1, R_2] = [NMe_2, NO_2]$ due to the larger donor strength of NMe_2. The reverse situation where R_1 is an acceptor and R_2 is a donor gives rise to a photoinduced electron delocalization from the benzopyrylium to the phenyl group, which has also for consequence the increase of the maximum absorption wavelength compared to the unsubstituted compound.

In all $\mathbf{AH}^+$ forms, a second band of higher energy is also observed. This latter has a weaker intensity than the low energy band, except in the compound where $R_1 = NMe_2$ and $R_2 = NO_2$. Note that in all compounds where a nitro group in the 4′ or 7-position is associated to a π-donor group in the other substitution center, the high and low energy bands have similar intensities.

The hydration reaction leading from $\mathbf{AH}^+$ to **Ct** is accompanied by either a hypso- or bathochromatic shift of the H $\rightarrow$ L band, depending on the nature of the substituents. A small blue shift is observed for compounds bearing a hydroxy or a methoxy group in R_1, whose importance increases when increasing the donor character of the susbstituent in R_2. In fact the internal CO group plays the role of an auxiliary acceptor and damps the effects of the donor groups, mainly those of R_1 because it is closer. On the contrary, compounds with $R_1 = NO_2$ display a red shift along the $\mathbf{AH}^+ \rightarrow \mathbf{Ct}$ reaction, the internal CO group reinforcing the attractor character of R_1, the 4′-nitro-7-dimethylamino-flavylium being associated to the largest red shift (−0.38 eV). Here also, this bathochromic displacement can be anticipated by considering the differences in the shape of the frontier orbitals: in **Ct** the HOMO and LUMO are localized on the opposite sides of the molecule, giving rise to a much larger photoinduced charge transfer than what is observed in $\mathbf{AH}^+$, and hence to a lower excitation energy. Finally, for compounds bearing an NMe_2 group in R_1, the change in the transition energy amounts to +0.38 eV for $R_2 = H$ and −0.14 eV for $R_2 = NO_2$.

Whatever the nature of the substituents in the 4′ and 7-positions, the $\mathbf{Ct} \rightarrow \mathbf{Ct}^-$ reaction is accompanied by a large bathochromic shift of the spectral band dominated by the H $\rightarrow$ L transition, which is particularly pronounced for compounds bearing a nitro acceptor group either in R_1 or R_2 (the larger shift attains 1.69 eV for the 4′-nitroflavylium).

5. Nonlinear Optical Properties

The static HRS first hyperpolarizabilities and depolarization ratios evaluated at different levels of approximation, that is, TDHF/6-31G(d) in vacuo and in acetonitrile, MP2/6-31G(d) in vacuo, are reported in Tables S3−S7. As usually observed for organic push−pull molecules,[2d,e,4] accounting for electron correlation at the MP2 level leads to an increase in the hyperpolarizability and DR values with respect to the CPHF results. The exaltation due to electron correlation depends on the nature of R_1 and R_2, and the β_{MP2}/β_{CPHF} ratios range from 0.97 to 1.72 for the $\mathbf{AH}^+$ forms, from 1.23 to 2.11 for the **Ct** forms, and from 2.06 to 3.01 for the $\mathbf{Ct}^-$ forms (see Table S7). Accounting for solvent effects also leads to an enhancement of the static β_{HRS} responses by roughly a factor of 2, which is less sensitive to the chemical species and to the nature of the substituents. This solvent-induced enhancement is substantially reduced when considering the dynamic β_{HRS} values, since the dynamic dielectric constant of acetonitrile is smaller than the static one, due to the lack of orientation term. As a consequence, the frequency dispersion factors calculated in the gas phase range from 1.30 to 2.61 depending on the substituents and on the chemical species, while they range from 0.7 to 1.4 in acetonitrile (see Table S5). On the contrary, the DR_{TDHF}/DR_{CPHF} ratios are slightly larger in acetonitrile than in gas phase. Finally, the HRS quantities calculated at the best level of approximation

TABLE 2: HRS First Hyperpolarizability (β_{HRS}, au) and Depolarization Ratios (DR) of Flavylium Derivatives Calculated at the IEFPCM/MP2/6-31G(d) Level in Acetonitrile

		$\lambda = \infty$					
		AH$^+$		**Ct**		**Ct$^-$**	
R_1	R_2	β_{HRS}	DR	β_{HRS}	DR	β_{HRS}	DR
H	H	2979	3.82	1877	3.91	7014	4.50
H	OH	3297	3.02	3506	4.22	7859	4.51
OH	H	6902	4.20	1736	2.75	6375	4.05
OH	OCH_3	7237	3.64	3043	3.40	7356	4.05
OH	OH	7149	3.67	3070	3.38	7287	4.15
OH	NH_2	7419	3.09	5202	3.91	8507	4.21
OH	NMe_2	7797	2.88	6752	4.04	8719	4.17
OH	NO_2	7912	4.62	1895	4.79	3110	3.27
OH	CN	7574	4.30	1459	2.90	5073	3.83
NMe_2	H	14998	4.41	3199	3.07	6104	3.36
NMe_2	NO_2	14981	4.71	5086	4.84	3386	2.58
OCH_3	H	7334	4.23	1731	2.80	6475	4.03
OCH_3	NO_2	8473	4.62	1910	4.69	3202	3.24
NO_2	H	1320	2.80	2882	4.98	11636	5.05
NO_2	NMe_2	4285	3.78	10478	4.79	15529	4.93
NO_2	OCH_3	2237	2.83	5051	4.82	12340	5.01
		$\lambda = 1064$ nm[a]					
H	H	2541	4.35	1757	4.61	7533	5.16
H	OH	2654	3.37	3331	4.87	8055	5.12
OH	H	6088	4.65	1448	2.98	6624	4.80
OH	OCH_3	6376	4.06	2827	3.98	7569	4.80
OH	OH	6162	4.13	2742	3.91	7251	4.83
OH	NH_2	6291	3.43	4916	4.52	8541	4.88
OH	NMe_2	7033	3.08	7110	4.75	9486	4.91
OH	NO_2	7524	4.96	1848	5.05	2522	3.52
OH	CN	7059	4.68	1207	2.94	5377	4.82
NMe_2	H	15718	4.81	2895	3.30	6196	3.89
NMe_2	NO_2	16854	4.97	5539	5.08	3179	3.28
OCH_3	H	6894	4.72	1478	3.03	6805	4.77
OCH_3	NO_2	8592	4.96	1935	4.95	2257	3.21
NO_2	H	888	2.92	3156	5.46	15266	5.33
NO_2	NMe_2	5245	4.21	12280	5.17	21011	5.22
NO_2	OCH_3	2233	3.60	5607	5.29	15906	5.31

[a] Dynamic values have been calculated using the multiplicative correction scheme.

achieved in this study, that is, IEFPCM/MP2/6-31G(d) in acetonitrile, are collected in the top of Table 2. The β_{HRS} and DR values including electron correlation, frequency dispersion, and solvent effects evaluated using eq 1 are given in the bottom of Table 2. Only these last values will be discussed in details.

Considering the **AH$^+$** cationic forms, it is noticeable that the HRS hyperpolarizabilities are much more affected by the substituent in R_1 than by the substituent in R_2, so that the compounds can be categorized with respect to the substituent in 4′ position. If one excepts the compound with $R_1/R_2 = NO_2/H$, the two compounds with no substitution in R_1 exhibit the smallest β_{HRS} responses. Grafting a hydroxy group in R_1 has for consequence to increase the β_{HRS} value by a factor of 2.4 compared to the nonsubstituted compound. Then, keeping $R_1 = OH$, the HRS hyperpolarizability can be enhanced by up to 24% by substitution in R_2, the largest values being obtained for the strongest acceptor (NO_2) or donor (NMe_2) groups. It is noteworthy that, although the impact of the R_2 substituent on β_{HRS} is limited, it widely affects the depolarization ratios, and thus the symmetry of the NLO-phore. Indeed, compounds bearing a strong acceptor group such as NO_2 or CN in R_2 have a more pronounced dipolar character and, thereof, DR values close to 5, while the compound with $R_2 = NMe_2$ has a DR close to 3. Replacing the hydroxy in R_1 by a stronger donor group (OCH_3 or NMe_2) further increases β_{HRS} as well as its dipolar character. In particular, compounds with $R_1 = NMe_2$ are associated to very high β_{HRS} values. Note that, although TDDFT calculations predict that the main absorption band of the 4′-dimethylamino-7-nitroflavylium cation (535 nm) is very close to the second harmonic wavelength (532 nm), the very large β_{HRS} values do not originate from resonance effects, since a similar effect is observed in the static case. Finally, grafting a nitro group in R_1 leads to a strong lowering of both β_{HRS} and DR, except for the DR value when R_2 is NMe_2.

SCHEME 2: Sketch of the Main Contributions to the First Hyperpolarizability of Flavylium-Type Derivatives[a]

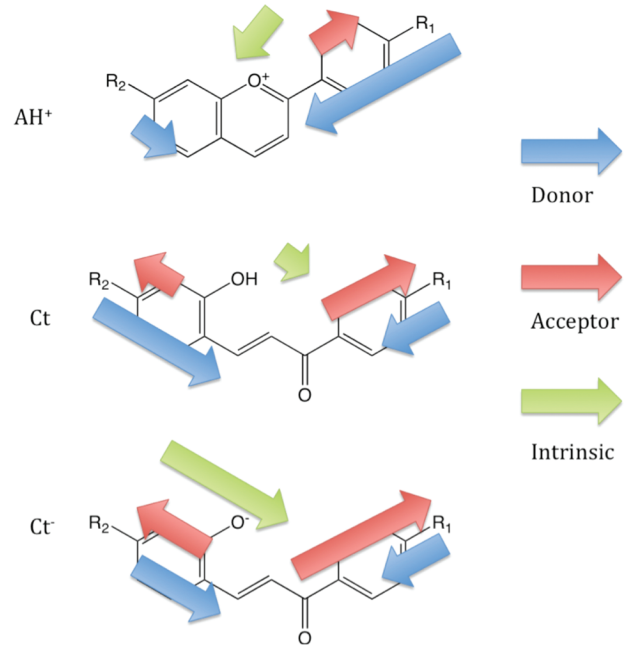

[a] For donor (red) and acceptor (blue) groups, the arrow points in the direction of the charge transfer (opposite to the change of dipole moment or to the first hyperpolarizability) whereas its amplitude is proportional to the susceptibility of the flavylium core to achieve a large β value in response to the donor or acceptor groups. So, a large arrow means that the first hyperpolarizability is strongly modified by the corresponding substituent and the stronger the donor/acceptor character, the larger the first hyperpolarizability contribution. In addition, the (green) arrow represents the intrinsic contribution of the flavylium core to the first hyperpolarizability.

For most of the R_1/R_2 pairs, the **Ct** form presents a weaker HRS response than the **AH$^+$** form, in relation with the hypsochromatic shift accompanying the **AH$^+$** → **Ct** reaction and with the decrease of the electron conjugation (i.e., the increase of BLA_1). On the contrary, as expected from the substantial bathochromatic shift, β_{HRS} increases from **AH$^+$** to **Ct** for the three compounds bearing a nitro group in R_1. These latter compounds also display a large increase of DR along the **AH$^+$** → **Ct** reaction, which reaches values from 5.17 to 5.46. On the absolute scale, β_{HRS} of the **Ct** form increases also when having a donor group in R_2 but this effect is not sufficient to overcome the large β_{HRS} of the corresponding **AH$^+$** forms, which is exalted by the donor groups in R_1.

Finally, the bathochromic shift **Ct** → **Ct$^-$** reaction has for consequence the increase of the HRS intensity, with the exception of the compound where $R_1/R_2 = NMe_2/NO_2$. In fact, β_{HRS} of the anion form is already large for $R_1/R_2 = H/H$ and it is further exalted by placing an acceptor in R_1 and, to a lesser extent, a donor in R_2.

The interplay between the nature of the substituents and the first hyperpolarizability is summarized in Scheme 2 for the **AH$^+$**,

TABLE 3: β_{HRS} Contrasts along the $AH^+ \rightarrow Ct$ and $Ct \rightarrow Ct^-$ Reactions

R_1	R_2	$AH^+ \rightarrow Ct$	$Ct \rightarrow Ct^-$
H	H	0.69	4.29
H	OH	1.26	2.42
OH	H	0.24	4.58
OH	OCH_3	0.44	2.68
OH	OH	0.45	2.64
OH	NH_2	0.78	1.74
OH	NMe_2	1.01	1.33
OH	NO_2	0.25	1.37
OH	CN	0.17	4.46
NMe_2	H	0.18	2.14
NMe_2	NO_2	0.33	0.57
OCH_3	H	0.21	4.60
OCH_3	NO_2	0.23	1.17
NO_2	H	3.55	4.84
NO_2	NMe_2	2.34	1.71
NO_2	OCH_3	2.51	2.84

Ct, and **Ct**$^-$ flavylium cores. In particular, Scheme 2 emphasizes the role of the different substituents—as well as of the core—to obtain large first hyperpolarizabilities. This is done using arrows, of which the length is proportional to the susceptibility of the flavylium core to achieve a large β value in response to the donor or acceptor groups. This further highlights that, when considering second-order NLO responses, flavylium compounds can be considered first as built from two moieties but that they can display cooperative effects when appropriately substituted.

As a key parameter of the efficiency of the various compounds for commutable NLO applications, the contrasts of β_{HRS} when switching between the different forms are reported in Table 3. With the exception of the compound with NMe_2/NO_2 in R_1/R_2, whose HRS response progressively decreases under the successive chemical transformations, the flavylium derivatives can be classified into two groups as a function of the evolution of β_{HRS} along the $\mathbf{AH^+ \rightarrow Ct \rightarrow Ct^-}$ path:

(1) Group A, where β_{HRS} increases along the $\mathbf{AH^+ \rightarrow Ct}$ and $\mathbf{Ct \rightarrow Ct^-}$ reactions.

(2) Group B, where β_{HRS} decreases along $\mathbf{AH^+ \rightarrow Ct}$ and then increases along the $\mathbf{Ct \rightarrow Ct^-}$ transformations.

Considering group A, the most efficient NLO switch is found to be the 4′-nitroflavylium derivative ($R_1 = NO_2$, $R_2 = H$), which exhibits contrasts as large as 3.55 and 4.84 along the two chemical transformations. In group B, three compounds display high β contrasts of ~0.2 along $\mathbf{AH^+ \rightarrow Ct}$ and of 4.5 for $\mathbf{Ct \rightarrow Ct^-}$ transformation: [R_1, R_2] = [OH, H], [OH, CN], [OCH_3, H].

6. Conclusions

The contrast of the second-order nonlinear optical response in flavylium derivatives has been investigated as a function of the nature of the substituents in the 4′- and 7-positions by means of quantum chemistry calculations including electron correlation, frequency dispersion, and solvent effects. These calculations show that the HRS hyperpolarizabilities and depolarization ratios are strongly dependent on the state of the compound and can be modulated by varying the nature of the chemical substituents. Considering the high contrasts of β_{HRS} along the $\mathbf{AH^+ \rightarrow Ct \rightarrow Ct^-}$ path obtained with specific combinations of substituents, these calculations demonstrate that flavylium derivatives can behave as highly efficient molecular NLO switches. The network of reversible chemical transformations based on these multistate/multifunctional systems can thus be taken as a basis in view of new logic devices for data processing and storage based on commutable NLO responses. It would now be very informative to see whether our theoretical predictions are confirmed experimentally.

Supporting Information Available: Representative structural parameters of the **AH**$^+$, **Cc**, **Ct**, and **Ct**$^-$ forms (Tables S1a−d), as well as calculated spectroscopic quantities (Table S2), frontiers MOs (Figure S1), simulated absorption spectra (Figure S2), and calculated HRS quantities (Tables S3−S7) for the three stable forms. This information is available free of charge via the Internet at http://pubs.acs.org.

Acknowledgment. E.B. thanks the European Commission through the EM ECW ("Erasmus Mundus External Cooperation Window") program for her Ph.D. grant. This work was supported by the Academy Louvain (ARC "Extended π-Conjugated Molecular Tinkertoys for Optoelectronics, and Spintronics"). The calculations have been performed on the Interuniversity Scientific Calculation Facility (ISCF) installed at the Facultés Universitaires Notre-Dame de la Paix (Namur, Belgium), for which the authors gratefully acknowledge the financial support of the F.R.S.-FRFC and the "Loterie Nationale" for the convention No. 2.4.617.07.F, and of the FUNDP, as well as on the "Mésocentre de Calcul Intensif Aquitain" (MCIA) financed by the Conseil Régional d'Aquitaine and the French Ministry of Research and Technology.

References and Notes

(1) (a) Coe, B. J. *Chem.—Eur. J.* **1999**, *5*, 2464. (b) Delaire, J. A.; Nakatani, K. *Chem. Rev.* **2000**, *100*, 1817. (c) Asselberghs, I.; Clays, K.; Persoons, A.; Ward, M. D.; McCleverty, J. *J. Mater. Chem.* **2004**, *14*, 2831.

(2) (a) Nakatani, K.; Delaire, J. A. *Chem. Mater.* **1997**, *9*, 2682. (b) Asselberghs, I.; Zhao, Y.; Clays, K.; Persoons, A.; Comito, A.; Rubin, Y. *Chem. Phys. Lett.* **2002**, *364*, 279. (c) Sliwa, M.; Létard, S.; Malfrant, I.; Nierlich, M.; Lacroix, P. G.; Asahi, T.; Matsuhara, H.; Yu, P.; Nakatani, K. *Chem. Mater.* **2005**, *17*, 4727. (d) Sliwa, M.; Nakatani, K.; Asahi, T.; Lacroix, P. G.; Pansu, R. B.; H. Masuhara, *Chem. Phys. Lett.* **2007**, *437*, 212. (e) Guillaume, M.; Champagne, B.; Markova, N.; Enchev, V.; Castet, F. *J. Phys. Chem. A* **2007**, *111*, 9914. (f) Plaquet, A.; Guillaume, M.; Champagne, B.; Rougier, L.; Mançois, F.; Rodriguez, V.; Pozzo, J.-L.; Ducasse, L.; Castet, F. *J. Phys. Chem. C* **2008**, *112*, 5638.

(3) Houbrechts, S.; Clays, K.; Persoons, A.; Pikramenou, Z.; Lehn, J. M. *Chem. Phys. Lett.* **1996**, *258*, 485.

(4) (a) Sanguinet, L.; Pozzo, J.-L.; Rodriguez, V.; Adamietz, F.; Castet, F.; Ducasse, L.; Champagne, B. *J. Phys. Chem. B* **2005**, *109*, 11139. (b) Mançois, F.; Rodriguez, V.; Pozzo, J.-L.; Champagne, B.; Castet, F. *Chem. Phys. Lett.* **2006**, *427*, 153. (c) Sanguinet, L.; Pozzo, J.-L.; Guillaume, M.; Champagne, B.; Castet, F.; Ducasse, L.; Maury, E.; Soulié, J.; Mançois, F.; Adamietz, F.; Rodriguez, V. *J. Phys. Chem. B* **2006**, *110*, 10672. (d) Mançois, F.; Sanguinet, L.; Pozzo, J.-L.; Guillaume, M.; Champagne, B.; Rodriguez, V.; Adamietz, F.; Ducasse, L.; Castet, F. *J. Phys. Chem. B* **2007**, *111*, 9795. (e) Mançois, F.; Pozzo, J. L.; Adamietz, F.; Rodriguez, V.; Ducasse, L.; Castet, F.; Plaquet, A.; Champagne, B. *Chem.—Eur. J.* **2009**, *15*, 2560.

(5) (a) McClelland, R. A.; Gedge, S. *J. Am. Chem. Soc.* **1980**, *102*, 5838. (b) McClelland, R. A.; McGall, G. H. *J. Org. Chem.* **1982**, *47*, 3730. (c) Pina, F. *J. Chem. Soc., Faraday Trans.* **1998**, *94*, 2109. (d) Pina, F.; Melo, M. J.; Parola, A. J.; Maestri, M.; Balzani, V. *Chem.—Eur. J.* **1998**, *4*, 2001. (e) Pina, F.; Lima, J. C.; Parola, A. J.; Afonso, C. A. M. *Angew. Chem., Int. Ed.* **2004**, *43*, 1525. (f) Ito, F.; Tanaka, N.; Katsuki, A.; Fujii, T. *J. Photochem. Photobiol. A* **2004**, *161*, 111. (g) Laia, C. A. T.; Parola, A. J.; Folgosa, F.; Pina, F. *Org. Biomol. Chem.* **2007**, *5*, 69.

(6) (a) Pina, F.; Melo, M. J.; Maestri, M.; Ballardini, R.; Balzani, V. *J. Am. Chem. Soc.* **1997**, *119*, 5556. (b) Pina, F.; Roque, A.; Melo, M. J.; Maestri, M.; Belladelli, L.; Balzani, V. *Chem.—Eur. J.* **1998**, *4*, 1184. (c) Pina, F.; Maestri, M.; Balzani, V. *Chem. Commun.* **1999**, 107.

(7) Giestas, L.; Folgosa, F.; Lima, J. C.; Parola, A. J.; Pina, F. *Eur. J. Org. Chem.* **2005**, 4187.

(8) (a) Pina, F.; Melo, M. J.; Maestri, M.; Passaniti, P.; Camaioni, N.; Balzani, V. *Eur. J. Org. Chem.* **1999**, 3199. (b) Maçanita, A. L.; Moreira, P. F., Jr.; Lima, J. C.; Quina, F. H.; Yihwa, C.; Vautier-Giongo, C. *J. Phys. Chem. A* **2002**, *106*, 1248. (c) Roque, A.; Lodeiro, C.; Pina, F.; Maestri, M.; Ballardini, R.; Balzani, V. *Eur. J. Org. Chem.* **2002**, 2699. (d) Moncada, M. C.; Fernández, D.; Lima, J. C.; Jorge Parola, A.; Lodeiro, C.; Folgosa, F.; Melo, M. J.; Pina, F. *Org. Biomol. Chem.* **2004**, *2*, 2802. (e) Roque, A.;

Lima, J. C.; Jorge Parola, A.; Pina, F. *Photochem. Photobiol. Sci.* **2007**, *6*, 381. (f) Horiuchi, H.; Tsukamoto, A.; Okajima, T.; Shirase, H.; Okutsu, T.; Matsushima, R.; Hiratsuka, H. J. *Photochem. Photobiol. A* **2009**, *205*, 203.

(9) Ito, F.; Tanaka, N.; Katsuki, A.; Fujii, T. *J. Photochem. Photobiol. A* **2002**, *150*, 153.

(10) Gomes, R.; Parola, A. J.; Lima, J. C.; Pina, F. *Chem.—Eur. J.* **2006**, *12*, 7906.

(11) Galindo, F.; Lima, J. C.; Luis, S. V.; Parola, A. J.; Pina, F. *Adv. Funct. Mater.* **2005**, *15*, 541.

(12) Gomes, R.; Parola, A. J.; Laia, C. A. T.; Pina, F. *Photochem. Photobiol. Sci.* **2007**, *6*, 1003. (b) Petrov, V.; Laia, C. A. T.; Pina, F. *Langmuir* **2009**, *25*, 594.

(13) Pina, F.; Hatton, T. A. *Langmuir* **2008**, *24*, 2356.

(14) (a) Pina, F.; Lima, J. C.; Parola, A. J.; Afonso, C. A. M. *Angew. Chem., Int. Ed.* **2004**, *43*, 1525. (b) Fernandez, D.; Parola, A. J.; Branco, L. C.; Afonso, C. A. M.; Pina, F. *J. Photochem. Photobiol.* **2004**, *168*, 185.

(15) (a) Sekino, H.; Bartlett, R. J. *J. Chem. Phys.* **1986**, *85*, 976. (b) Karna, S. P.; Dupuis, M. *J. Comput. Chem.* **1991**, *12*, 487–504.

(16) (a) Tomasi, J.; Persico, M. *Chem. Rev.* **1994**, *94*, 2027. (b) Tomasi, J.; Mennucci, B.; Cammi, R. *Chem. Rev.* **2005**, *105*, 2999.

(17) Cohen, H. D.; Roothaan, C. C. J. *J. Chem. Phys.* **1965**, *43*, S34.

(18) (a) Davis, P. J.; Rabinowitz, P. In Numerical Integration; Blaisdell Publishing Company: London, 1967; p 166. (b) See also for an example of the Romberg scheme in the case of push-pull π-conjugated systems, Champagne, B.; Kirtman, B. *Nonlinear Optical Materials*; Nalwa, H. S. Ed.; Handbook of Advanced Electronic and Photonic Materials and Devices; Academic Press: San Diego, 2001; Vol. 9, Ch. 2, p 63.

(19) Champagne, B.; Kirtman, B. *J. Chem. Phys.* **2006**, *125*, 024101.

(20) Verbiest, T.; Clays, K.; Rodriguez, V. *Second-Order Nonlinear Optical Characterizations Techniques: An Introduction*; CRC Press: New York, 2009.

(21) Bersohn, R.; Pao, Y. H.; Frisch, H. L. *J. Chem. Phys.* **1966**, *45*, 3184.

(22) Yang, M.; Champagne, B. *J. Phys. Chem. A* **2003**, *107*, 3942.

(23) Frisch, M. J.; Trucks, G. W.; Schlegel, H. B.; Scuseria, G. E.; Robb, M. A.; Cheeseman, J. R.; Montgomery, J. A.; Vreven, T.; Kudin, K. N.; Burant, J. C.; Millam, J. M.; Iyengar, S. S.; Tomasi, J.; Barone, V.; Mennucci, B.; Cossi, M.; Scalmani, G.; Rega, N.; Petersson, G. A.; Nakatsuji, H.; Hada, M.; Ehara, M.; Toyota, K.; Fukuda, R.; Hasegawa, J.; Ishida, M.; Nakajima, T.; Honda, Y.; Kitao, O.; Nakai, H.; Klene, M.; Li, X.; Knox, J. E.; Hratchian, H. P.; Cross, J. B.; Bakken, V.; Adamo, C.; Jaramillo, J.; Gomperts, R.; Stratmann, R. E.; Yazyev, O.; Austin, A. J.; Cammi, R.; Pomelli, C.; Ochterski, J. W.; Ayala, P. Y.; Morokuma, K.; Voth, G. A.; Salvador, P.; Dannenberg, J. J.; Zakrzewski, V. G.; Dapprich, S.; Daniels, A. D.; Strain, M. C.; Farkas, O.; Malick, D. K.; Rabuck, A. D.; Raghavachari, K.; Foresman, J. B.; Ortiz, J. V.; Cui, Q.; Baboul, A. G.; Clifford, S.; Cioslowski, J.; Stefanov, B. B.; Liu, G.; Liashenko, A.; Piskorz, P.; Komaromi, I.; Martin, R. L.; Fox, D. J.; Keith, T.; Al-Laham, M. A.; Peng, C. Y.; Nanayakkara, A.; Challacombe, M.; Gill, P. M. W.; Johnson, B.; Chen, W.; Wong, M. W.; Gonzalez, C.; Pople, J. A. *Gaussian 03, Revision C.02*; Gaussian, Inc.: Wallingford CT, 2004.

JP1056804